Regulatory Tasks of the Phosphoenolpyruvate-Phosphotransferase System of *Pseudomonas putida* in Central Carbon Metabolism

Max Chavarría,[a] Roelco J. Kleijn,[b] Uwe Sauer,[b] Katharina Pflüger-Grau,[a]* and Víctor de Lorenzo[a]

Systems Biology Program, Centro Nacional de Biotecnología (CNB-CSIC), Cantoblanco-Madrid, Spain,[a] and Institute of Molecular Systems Biology, ETH Zurich, Zurich, Switzerland[b]

* Present address: Fachgebiet Systembiotechnologie, Technische Universität München, Munich, Germany.

ABSTRACT **Two branches of the phosphoenolpyruvate-phosphotransferase system (PTS) operate in the soil bacterium *Pseudomonas putida* KT2440. One branch encompasses a complete set of enzymes for fructose intake (PTS^{Fru}), while the other (N-related PTS, or PTS^{Ntr}) controls various cellular functions unrelated to the transport of carbohydrates. The potential of these two systems for regulating central carbon catabolism has been investigated by measuring the metabolic fluxes of isogenic strains bearing nonpolar mutations in PTS^{Fru} or PTS^{Ntr} genes and grown on either fructose (a PTS substrate) or glucose, the transport of which is not governed by the PTS in this bacterium. The flow of carbon from each sugar was distinctly split between the Entner-Doudoroff, pentose phosphate, and Embden-Meyerhof-Parnas pathways in a ratio that was maintained in each of the PTS mutants examined. However, strains lacking PtsN ($EIIA^{Ntr}$) displayed significantly higher fluxes in the reactions of the pyruvate shunt, which bypasses malate dehydrogenase in the TCA cycle. This was consistent with the increased activity of the malic enzyme and the pyruvate carboxylase found in the corresponding PTS mutants. Genetic evidence suggested that such a metabolic effect of PtsN required the transfer of high-energy phosphate through the system. The $EIIA^{Ntr}$ protein of the PTS^{Ntr} thus helps adjust central metabolic fluxes to satisfy the anabolic and energetic demands of the overall cell physiology.**

IMPORTANCE **This study demonstrates that $EIIA^{Ntr}$ influences the biochemical reactions that deliver carbon between the upper and lower central metabolic domains for the consumption of sugars by *P. putida*. These findings indicate that the $EIIA^{Ntr}$ protein is a key player for orchestrating the fate of carbon in various physiological destinations in this bacterium. Additionally, these results highlight the importance of the posttranslational regulation of extant enzymatic complexes for increasing the robustness of the corresponding metabolic networks.**

Received 29 January 2012 **Accepted** 2 February 2012 **Published** 20 March 2012

Citation Chavarría M, Kleijn RJ, Sauer U, Pflüger-Grau K, and de Lorenzo V. 2012. Regulatory tasks of the phosphoenolpyruvate-phosphotransferase system of *Pseudomonas putida* in central carbon metabolism. mBio 3(2):e00028-12. doi:10.1128/mBio.00028-12.

Editor E. Peter Greenberg, University of Washington

Address correspondence to: Víctor de Lorenzo, vdlorenzo@cnb.csic.es.

Coordinating the uptake and the fluxes of C compounds through central metabolic pathways to generate biosynthetic precursor metabolites is essential for bacterial cell growth (1). This requires multilevel control of the expression and activity of the proteins involved. Transcriptional regulation of biochemical networks is orchestrated through the action of flux-sensing transcriptional factors (2, 3) and small RNAs (4), but often, short-term physiological needs may demand faster, coordinated changes in the activity of already expressed enzymes and related proteins. Phosphorylation is a widespread mechanism for this process, as it affords instant changes in protein activity (5, 6) and allows the channeling of specific signals through the otherwise diffusible medium of the cytoplasm (5). The phosphoenolpyruvate-carbohydrate phosphotransferase system (PTS) is one of the key players in such a nongenetic control of physiological and metabolic activities (7, 8) in both Gram-negative and Gram-positive bacteria. The PTS includes an array of phosphotransferase activities borne by the proteins EI, HPr, EIIA, and EIIB(C), which may occur as separate polypeptides or as hybrid fusions. EI acquires phosphate from phosphoenolpyruvate (PEP) and subsequently passes it to HPr, and then the phosphorylated HPr (P~HPr) passes it to EIIABC (8, 9). In the canonical system, the ultimate acceptor of the phosphate is a sugar that becomes phosphorylated by the permease component of the phosphotransfer chain, EIIBC, as it is transported into the cell. The variable PEP/pyruvate ratio that is generated as available sugars are metabolized (8) determines the distribution of phosphorylated versus nonphosphorylated forms of the PTS proteins. These components then signal the metabolic state of the cells to multiple targets by means of protein-protein interactions (8–10).

In the soil bacterium *Pseudomonas putida*, one sugar-specific PTS for fructose transport comprising FruB (EI-HPr-EIIA) and FruA (EIIBC) coexists with an alternative paralogous protein set ($PtsP/EI^{Ntr}$, PtsO/NPr, and $PtsN/EIIA^{Ntr}$), which lacks the EIIBC modules for sugar uptake (Fig. 1). The functions of the alternative PTS in *P. putida* and other bacteria are uncertain. While it was first believed to be a sensor of the metabolic balance between N and C (11–13), more recent results suggest that it controls also the influx

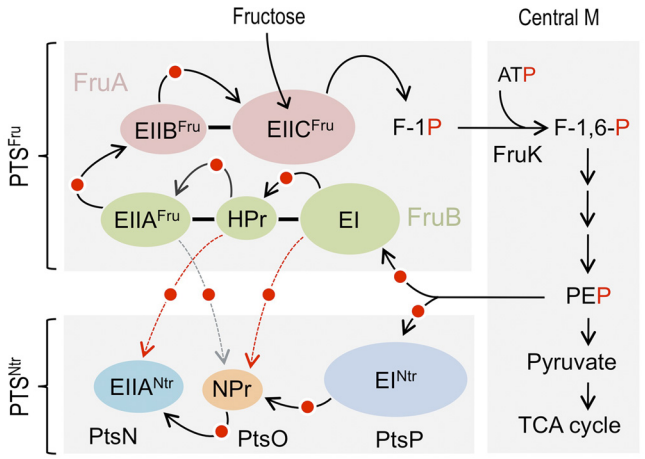

FIG 1 Organization and interplay of the fructose-related and N-related branches of the *P. putida* PTS. (Top left) Components of PTS^{Fru}, which includes the membrane-bound permease FruA, consisting of a fusion of EIIB^{Fru} and EIIC^{Fru} domains. It is generally believed that P-EIIB phosphorylates the carbohydrate bound to EIIC. FruA thus transports extracellular fructose through a phosphorylation-dependent process to yield fructose 1-P (F1P), which is then channeled towards the central metabolism following the action of FruK to yield fructose 1,6-bisphosphate (FBP). The second component of the PTS^{Fru} is FruB, a fusion of EIIA^{Fru}, HPr, and EI modules into a single polypeptide, the last domain of which is responsible for conveying high-energy phosphates from phosphoenolpyruvate (PEP) into the system. The flow of such phosphate through each of the constituents of the system is indicated. (Bottom left) PTS^{Ntr}, which is composed of the proteins PtsN (EIIA^{Ntr}), PtsO (NPr), and PtsP (EI^{Ntr}). The transfer of phosphate from PEP among them is shown, although EIIA^{Ntr}~P lacks any plausible EIIBC counterpart. The arrows between the two PTS branches represent the known cross talk between them (21). Note also that PEP is the shared ultimate donor of phosphate for the two systems.

and efflux of potassium ions (14). However, the initial designation of PTS^{Ntr} (15) has been maintained in the relevant literature, and we use it in this article. Despite the ambiguity regarding the signals that PTS^{Ntr} responds to, the phenotypes of mutants lacking the corresponding proteins indicate that it controls, directly or indirectly, a variety of metabolic functions (14, 16–20). Moreover, both *in vitro* (15) and *in vivo* (21, 22) evidence indicates that the sugar-related PTS and the PTS^{Ntr} have a degree of cross talk (Fig. 1), thus suggesting that the entire PTS network is a major protein-based device for controlling a suite of metabolic processes. However, how can such a hypothesis be tested?

In this work, we exploited the known interplay between the different components of the PTS of *P. putida* (Fig. 1) for examining the influence of its constituents on central metabolism. To this end, we determined ^{13}C metabolic fluxes in isogenic *P. putida* strains carrying single or multiple nonpolar mutations in components of the phosphotransferase systems, grown either on a PTS sugar (fructose) or a non-PTS substrate (glucose). Our data indicate that the PTS^{Ntr} influences the flow of carbon to and from the tricarboxylic acid (TCA) cycle by downregulating the shunt that converts malate to pyruvate. Furthermore, the metabolic phenotypes of the various PTS mutants suggested that such a regulatory action relies on the phosphorylation state of the EIIA^{Ntr} component of the complex in a manner that is dependent on the cross talk between the two branches of the phosphotransferase system in this bacterium. We argue that such a control allows virtually immediate adaptation of the central metabolism of *P. putida* to changes in the nutrients available in the medium.

RESULTS

Growth of *P. putida* on PTS versus non-PTS sugars. While glucose and fructose are similar hexoses with virtually identical energy values, they are predicted to follow different routes into the central metabolism of *P. putida* (23). Glucose can be transported through a dedicated ABC uptake system (involving PP1015 to PP1018) (24) into the cytoplasm, where it is phosphorylated to glucose 6-phosphate (G6P) and, further, to 6P-gluconate (Fig. 2). Alternatively, glucose can also diffuse into the periplasm and be converted there to gluconate and then to 2-ketogluconate. Both of these intermediates are then transported into the cytoplasm to be transformed into 6P-gluconate and to 2-keto-6-phosphogluconate, which is itself converted to 6P-gluconate. Note that regardless of such events, all upstream intermediates from glucose converge towards 6P-gluconate, which can then enter either the Entner-Doudoroff (ED) pathway or the pentose phosphate (PP) pathway (25) (Fig. 2). In contrast, fructose is imported through a typical PTS permease (FruA) consisting of a fusion of EIIB^{Fru} and EIIC^{Fru} domains. Fructose is thus converted first to fructose 1-phosphate (F1P) and then to fructose 1,6-bisphosphate, which, according to the current metabolic models (26, 27), can next enter the ED pathway and/or a standard glycolytic Embden-Meyerhof-Parnas (EMP) route (Fig. 2). Despite these differences in the earlier stages of their metabolism, glucose and fructose ultimately converge into the production of phosphoenolpyruvate (PEP) and pyruvate as the point of entry into the TCA cycle. The major functions of all these central pathways include generating not only biosynthetic precursor metabolites but also NADPH for biosyntesis, NADH for energy, and reductive power to deal with both environmental and endogenous oxidative stress (26, 27).

The first question of interest was whether growth on a particular sugar influenced the overall physiology of wild-type *P. putida* MAD2. Inspection of the growth parameters of Table 1 indicates that during the exponential phase, bacteria grew on fructose ~60% more slowly than on glucose. As shown in Table 1, the inferior growth rate on fructose was consistent with a slower uptake of the carbohydrate (~0.75 mmol sugar/g biomass/hour). In contrast, cells grown on glucose consumed the sugar >6-fold faster (~4.79 mmol glucose/g biomass/hour). These differences in growth parameters (Table 1) suggested that cells might not only channel each of these sugars through different pathways but also adapt to different overall metabolic regimens. To study this possibility, the flow of carbon from each of these sugars through the central metabolic routes (Fig. 2) was inspected as described below.

Glucose and fructose meet different metabolic fates in *P. putida*. The carbon fluxes of cells growing in either glucose or fructose were calculated in steady-state cultures as described in Materials and Methods. First, using ^{13}C-labeled substrates, we calculated the flux ratios (see Fig. S1 in the supplemental material). These ratios were then used as constraints in a stoichiometric reaction model for the estimation of intracellular carbon fluxes (net fluxes) at 16 sites of the metabolic network (Fig. 2). For the sake of the analysis, the central biochemical landscape following the uptake of the carbohydrate (Fig. 2) can be grossly differentiated into an upper domain (i.e., the EMP, ED, and PP pathways) for the breakdown of the hexoses into C_3 compounds (pyruvate and

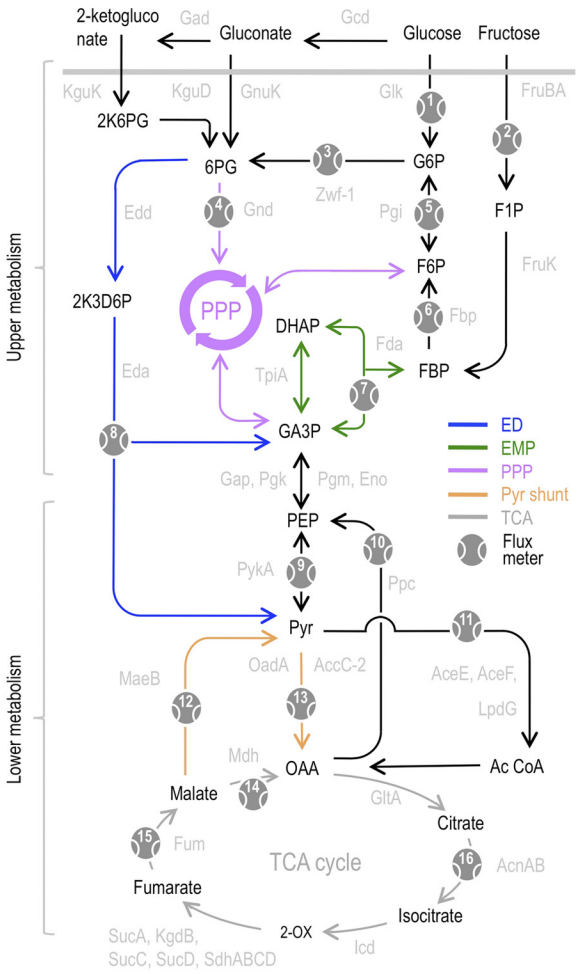

FIG 2 Glucose and fructose metabolism in *P. putida*. The scheme summarizes the network of reactions in cells growing on either sugar as the sole carbon source. The upper metabolic domain comprises the Entner-Doudoroff (ED) pathway, the Embden-Meyerhof-Parnas (EMP) glycolytic route and the pentose phosphate pathway (PPP, represented as a cycle). The lower metabolic domain encompasses the phosphoenolpyruvate-pyruvate-oxaloacetate (PEP-Pyr-OAA) node, including the pyruvate shunt and the TCA cycle. The metabolites involved in each of the corresponding transformations are indicated: G6P, glucose 6-phosphate; F1P, fructose 1-phosphate; FBP, fructose 1,6-bisphosphate; 6PG, 6-phosphogluconate; 2K6PG, 2-keto-6-phosphogluconate; 2K3D6P, 2-keto-3-deoxy-6-phosphogluconate; GA3P, glyceraldehyde 3-phosphate; DHAP, dihydroxyacetone phosphate; PEP, phosphoenolpyruvate; Pyr, pyruvate; AcCoA, acetyl-CoA; OAA, oxaloacetate; 2-OX, 2-oxoglutarate. The enzymes that catalyze each of the transformations are shown with the corresponding ORF code from the *P. putida* genome: FruBA, permease/phosphotransferase system for fructose (23); Pgi, glucose-6-phosphate isomerase (PP_1808); Fbp, fructose 1,6-bisphosphate phosphatase (PP_5040); Fda, fructose 1,6-bisphosphate aldolase (PP_4960); Zwf-1, glucose 6-phosphate 1-dehydrogenase (PP_1022); Edd, phosphogluconate dehydratase (PP_1010); Eda, keto-hydroxyglutarate-aldolase (PP_1024); TpiA, triosephosphate isomerase (PP_4715); Gap, glyceraldehyde-3-phosphate dehydrogenase (PP_1009); Pgk, phosphoglycerate kinase (PP_4963); Pgm, phosphoglyceromutase (PP_5056); Eno, phosphopyruvate hydratase (PP_1612); PykA, pyruvate kinase (PP_1362); AceE, pyruvate dehydrogenase subunit E1 (PP_0339); AceF, dihydrolipoamide acetyltransferase (PP_0338); LpdG, dihydrolipoamide dehydrogenase (PP_4187); GltA, citrate synthase (PP_4194); AcnA, aconitate hydratase 1 (PP_2112); AcnB, aconitate hydratase 2 (PP_2339); Icd, isocitrate dehydrogenase (PP_4011); Kgd, alpha-ketoglutarate decarboxylase (PP_4189); KgdB, dihydrolipoamide acetyltransferase (PP_4188); SucA, 2-oxoglutarate dehydrogenase E1 component (PP_4189); SucC, succinyl-CoA synthetase beta subunit (PP_4186); SucD, succinyl-CoA synthetase (PP_4185); SdhA, succinate dehydrogenase flavoprotein subunit (PP_4191); SdhB, succinate dehydrogenase iron sulfur subunit (PP_4190); SdhC, succinate dehydrogenase, cytochrome b556 subunit (PP_4193); SdhD, succinate dehydrogenase, hydrophobic membrane anchor protein (PP_4192); Fum, fumarate hydratase (PP_0897); Mdh, malate dehydrogenase (PP_0654); OadA, pyruvate carboxylase subunit B (PP_5346); AccC-2, pyruvate carboxylase subunit A (PP_5347); MaeB, malic enzyme (PP_5085); Ppc, phosphoenolpyruvate carboxylase (PP_1505). The 16 sites of the network where metabolic fluxes could be calculated as explained in the text are indicated.

phosphoenolpyruvate) and a lower domain that encompasses the phosphoenolpyruvate-pyruvate-oxaloacetate (PEP-Pyr-OAA) checkpoint node and the TCA cycle. Figure 3 shows the division of carbon fluxes (i.e., relative values normalized to the amount of the imported C source) through the upper metabolic domain of *P. putida*. As expected (25), the bulk (~96%) of glucose was metabolized via the ED pathway to pyruvate, while the other ~4% of the sugar was channeled into the PP route (Fig. 3). Also as anticipated, no signs of glycolytic activity were detected, as *P. putida* lacks the phosphofructokinase activity that directs F6P into the EMP pathway (23). The fate of fructose was, however, altogether different. Although this sugar can undergo complete glycolysis through the

TABLE 1 Physiological characteristics of *P. putida* MAD2 and its *pts* mutants grown on glucose or fructose as the sole C source

C source and strain or genotype	Maximum specific growth rate (h^{-1})	Biomass yield ($y_{x/substrate}$) ($g_{CDW}/g_{substrate}$)	Specific substrate consumption rate ($mmol_{substrate}/g_{biomass}/h$)
Glucose			
MAD2	0.25 ± 0.01	0.28 ± 0.03	4.79 ± 0.38
fruB	0.30 ± 0.02	0.29 ± 0.04	4.75 ± 0.43
ptsO	0.30 ± 0.01	0.32 ± 0.02	4.86 ± 0.32
ptsP	0.32 ± 0.03	0.29 ± 0.01	4.90 ±0.43
ptsN	0.23 ± 0.01	0.25 ± 0.04	4.20 ± 0.25
ptsN/ptsO	0.21 ± 0.01	0.31 ± 0.03	4.10 ± 0.11
ptsP/fruB	0.27 ± 0.02	0.31 ± 0.02	4.38 ± 0.10
Fructose			
MAD2	0.15 ± 0.05	0.47 ± 0.01	0.85 ± 0.04
fruB	Not applicable		
ptsO	0.12 ± 0.03	0.55 ± 0.01	0.96 ± 0.03
ptsP	0.13 ± 0.02	0.47 ± 0.03	0.80 ± 0.03
ptsN	0.09 ± 0.04	0.49 ± 0.09	0.87 ± 0.02
ptsN/ptsO	0.11 ± 0.03	0.45 ± 0.01	0.90 ± 0.01
ptsP/fruB	Not applicable		

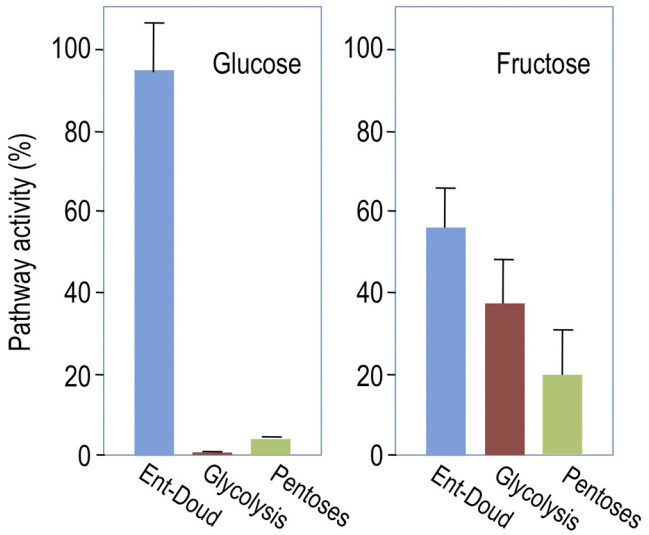

FIG 3 Channeling of glucose and fructose through each of the upstream sugar-catabolic pathways. The activities on the *y* axes represent the net fluxes of carbon through each of the routes calculated using metabolic flux analysis of *P. putida* MAD2 grown on the compound indicated in each case (see the text and Fig. S1). Note that *P. putida* degrades glucose mainly through the Entner-Doudoroff (ED) pathway (~96%). Fructose is also catabolized mostly by the ED route (52%) but with an important contribution from standard glycolysis (the Embden-Meyerhof-Parnas [EMP] pathway), which accounts for ~34% of the corresponding flux.

EMP pathway, only ~34% of the sugar was channeled through this route. The majority of fructose (~52%) was instead diverted to the ED pathway and the rest (~14%) to the PP route. Considering that *P. putida* is endowed with an entire complement of enzymes for channeling fructose through either the EMP or the ED pathway, it came as a surprise that most of the sugar was still metabolized through a less energetically favorable route (28). Regardless, these data revealed considerable divergences in the early metabolism of two otherwise similar carbohydrates. However, the final products of the upper metabolism of both sugars were the same: PEP and pyruvate. Accordingly, the next question was whether the further metabolism of these 3C compounds (i.e., their entry into the TCA cycle) (Fig. 2) was independent of how they were generated.

The function of the upper metabolic domain determines the mode of access of 3C compounds to the TCA cycle. An examination of the carbon fluxes in cells grown on each of the two sugars studied revealed considerable differences through the lower metabolic domain, particularly through the PEP-Pyr-OAA node (Fig. 4a). First, cells grown on fructose had a significantly higher gluconeogenic flux from OAA back to PEP catalyzed by the phosphoenolpyruvate carboxylase (Ppc) enzyme. As shown in Fig. 4b, cells grown on fructose had ~16% of the PEP derived from OAA (via Ppc), ~36% from the ED pathway (via Edd/Eda), and 48% generated via the EMP pathway. In contrast, bacteria consuming glucose had only ~7% of their PEP derived from OAA and the rest (~93%) from the ED pathway. A second remarkable difference at the lower metabolism boundary was that the pool of OAA originated directly from malate via malate dehydrogenase (Fig. 4b) during growth on each sugar. We could calculate that in fructose, ~48% of OAA came from malate, a figure that increased to 65% in the case of cells grown on glucose. Moreover, the flux from pyruvate to OAA (catalyzed by Acc-2/OadA) (Fig. 4a) was 1.5-fold lower in glucose-grown cells than in fructose-grown cells. Comparison of the origins of the pyruvate pool (Fig. 4b) under the two growth conditions indicated that ~20% of this metabolite resulted from the activity of the malic enzyme (MaeB) and ~60% directly from PEP (via PykA) in cells growing in fructose. These figures diverge from those corresponding to cells grown on glucose, as the breakdown of the pyruvate pool is, in this case, ~9% from malate and 43% from PEP. Therefore, the pyruvate shunt (Fig. 4a) is more active during growth on fructose. The increase of the downward flux of PEP→pyruvate on fructose is likely to stem from the different routes that either sugar followed to that point. As mentioned above, the portion of the fructose that goes through the EMP pathway yields PEP as the primary metabolic product, thus providing more substrate for its conversion to pyruvate and increasing the corresponding flux. In contrast, because most glucose goes through the ED route, a significant portion of the pyruvate is derived directly from the activity of the ED pathway (~48% in glucose versus ~20% on fructose) (Fig. 4b).

The divergent routes of glucose and fructose immediately after their uptake could easily explain the differences found in the upper metabolism of each sugar. However, these differences at the PEP-Pyr-OAA node suggest that another actor(s) may control the performance of such a link between glycolysis, gluconeogenesis, and the TCA cycle (Fig. 2). This node acts as a major divider of carbon fluxes among catabolism, anabolism, and the energy supply of the cell (29). Even small differences in this node's performance have consequences for the overall metabolic homeostasis (30). Because the only conspicuous difference between the metabolism of the two sugars following production of PEP or pyruvate is their relation to the PTS, we questioned whether any of their phosphotransferases could have a role in setting the different metabolic regimens of cells growing on each of these substrates.

The PTS of *P. putida* modulates the connection between the upper and the lower sugar metabolic domains. The effect of various components of the PTS of *P. putida* on the function of both the upper and the lower metabolic domains was examined. To this end, we employed an isogenic collection of *P. putida* strains bearing single-knock-out, nonpolar mutations (see Materials and Methods) in the genes *ptsN*, *ptsO*, *ptsP*, and *fruB* (Fig. 1), as well as the double mutations *ptsN ptsO* and *ptsP fruB*. Because the route of high-energy phosphate through the corresponding PTS proteins is known (21, 31) (Fig. 1), the phosphorylation state of the relevant proteins can be predicted for each of the mutants. Using these strains, we determined the flux of carbon through both the upper and the lower metabolic domains of each of the PTS mutants grown on either glucose or fructose. The results (see Fig. S1 in the supplemental material) immediately indicated that none of the *pts* mutations had a significant influence on the fluxes through the upper metabolic domain of cells growing on either sugar, with the anticipated exception of *fruB* mutants, which cannot grow on fructose (19). We did observe, however, a number of significant changes in the downstream reactions (i.e., the PEP-Pyr-OAA node). In all cases, the absence of PtsN ($EIIA^{Ntr}$) was systematically associated with changes in flux distributions. The corresponding net fluxes of the other mutants (*fruB*, *ptsP*, *ptsO*, and *fruB ptsP*) were indistinguishable from those of the wild-type on either of the sugars (data not shown) and were not considered in the subsequent analyses. In contrast, as shown in Fig. S2 and Fig. S3 in the supplemental material, strains lacking *ptsN* displayed higher fluxes in the reactions of the pyruvate shunt,

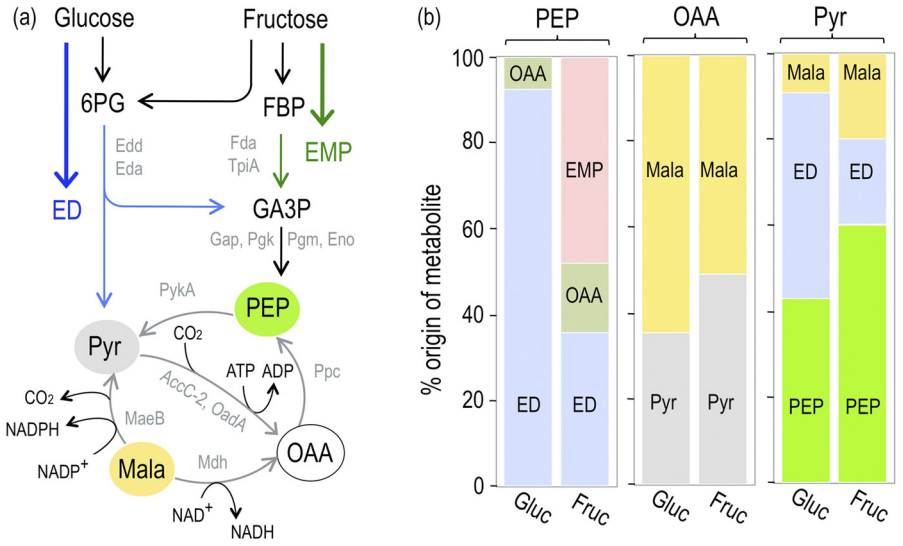

FIG 4 The origin of the components of the phosphoenolpyruvate-pyruvate-oxaloacetate (PEP-Pyr-OAA) node. (a) Major biochemical reactions that connect the ED and EMP routes with the malate and oxaloacetate components of the Krebs cycle. The routes necessary for the conversion of glucose and fructose into metabolic currency (Pyr and PEP) are illustrated on top along with the enzymes that belonging to the ED or the EMP pathways. The bottom highlights the reactions at the boundary between the upper and the lower metabolic domains, including the PEP-Pyr-OAA node and the Pyr shunt. (b) A breakdown of the route of key metabolites (PEP, OAA, and pyruvate) through each of the connecting reactions of the upper and lower metabolic boundaries for either glucose or fructose. The percentage of each precursor compound or pathway is indicated in every case: PEP derived from the EMP pathway, from the ED pathway, or from OAA (via phosphoenolpyruvate carboxylase [Ppc]); OAA directly from malate (via malate dehydrogenase [Mdh]) or from pyruvate (through pyruvate carboxylase [AccC-2/OadA]); and pyruvate derived from malate (via malic enzyme [MaeB]), directly from the ED pathway (Eda enzyme) or from PEP (via the pathway GA3P→PEP→Pyr).

malate→pyruvate→OAA (fluxes 12 and 13) (Fig. 2), regardless of the C source employed for growth. These changes, which were detected in the flux ratios (see Fig. S1), became more noticeable when represented as net fluxes (see Fig. S2 and Fig. S3). These values allow a reliable comparison between different strains because the data are normalized to hexose consumption (see Materials and Methods). As shown in Fig. S2 and Fig. S3, the flux from pyruvate to OAA catalyzed by the pyruvate carboxylase (flux 13) increased in the *ptsN* mutant ~1.2-fold on glucose (~1.4-fold in the *ptsN ptsO* strain) and ~1.4-fold on fructose (~1.5-fold in the *ptsN ptsO* mutant). Similarly, the flux from malate to pyruvate (flux 12) caused by the malic enzyme increased in the *ptsN* strain ~1.6-fold on glucose (~2.3-fold in the *ptsN ptsO* mutant) and ~1.5-fold on fructose (~1.7-fold in the *ptsN ptsO* strain). The loss of the PtsN protein thus led, on average, to a 1.6-fold increase in the carbon fluxes of the reactions of the pyruvate shunt. Despite these relatively modest changes, statistical analyses (*t* tests) demonstrated that the differences in the fluxes of the wild-type strain versus the those in the *ptsN* and *ptsN ptsO* mutants were all significant at a confidence level of ≥95%, with the exception of the single *ptsN* mutant on glucose. This does not, however, change the conclusion, because the single *ptsN* mutant was the only case where fluxes during growth on glucose were clearly higher than those in the wild-type strain. Moreover, the *ptsN* mutant also presented higher flux distributions in the TCA cycle than the parental strain when grown on fructose. Because both glucose and fructose resulted in an increase of the activity of the pyruvate shunt in the absence of PtsN, we decided to confirm this observation with enzymatic assays.

PtsN downregulates the activity of the enzymes of the pyruvate shunt. As discussed above, strains lacking PtsN displayed significantly higher fluxes through the pyruvate shunt, which bypasses malate dehydrogenase in the TCA cycle, thus converting malate directly to pyruvate (see Fig. S2 and Fig. S3 in the supplemental material). From a biochemical perspective, this shunt comprises the reaction malate→pyruvate (see above) and a subsequent step, pyruvate→oxaloacetate, executed by the pyruvate carboxylase. Note that the last enzyme catalyzes the addition of a carboxyl group to pyruvate (using CO_2) (Fig. 4a) to make oxaloacetate. Analysis of the chemical reactions involved in the pyruvate shunt indicates that it is energetically costly (due to the ATP hydrolysis by pyruvate carboxylase) but possibly useful for the redox balance, as it creates NADPH via the malic enzyme. To shed light on this question, the effect of PtsN was separately examined in each of the enzymatic steps that form the shunt.

The genome of *P. putida* possesses only one candidate gene able to encode the malic enzyme: *maeB* (PP_5085). In contrast, *P. aeruginosa* has two equivalent activities that differ in cofactor preference (NAD^+ or $NADP^+$) (32). In *P. putida*, two genes encode the corresponding subunits of pyruvate carboxylase: *accC-2* (PP_5347) and *oadA* (PP_5346). To determine whether the effect of PtsN ($EIIA^{Ntr}$) on the pyruvate shunt reflects a direct or indirect action of the phosphotransferase on its constituent enzymatic activities, cell-free extracts were prepared from wild-type *P. putida* and from the *ptsN* and *ptsN ptsO* mutants after growth on either fructose or glucose. The protein samples were then assayed for activity of the malic enzyme and pyruvate carboxylase as explained in Materials and Methods, with the results shown in Fig. 5. Note that the only measurable activity of the malic enzyme was NADP-dependent, not NAD-dependent. This confirmed the presence of a single isoenzyme, likely encoded by *maeB*. Figure 5 shows that such an activity was higher in cell extracts devoid of

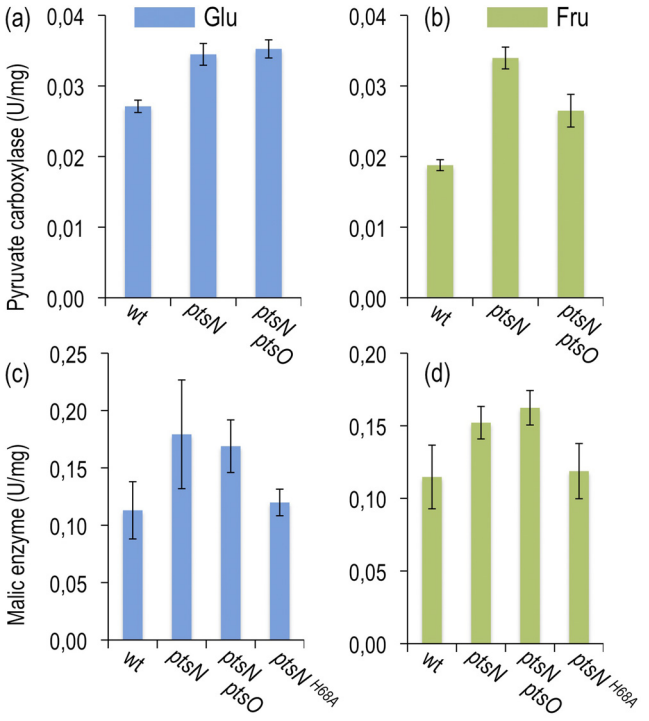

FIG 5 Activity of the enzymes of the pyruvate shunt in extracts of wild-type *P. putida* MAD2 and *ptsN* mutants. (a and b) Activity of pyruvate carboxylase in *P. putida* MAD2 (wt) and its *ptsN* and *ptsN ptsO* variants in cells grown on glucose (a) and on fructose (b). (c and d) Activity of the malic enzyme in *P. putida* MAD2 (wt) and *ptsN*, *ptsN ptsO*, and *ptsN*(*H68A*) mutants grown on glucose (c) and on fructose (d). The levels of pyruvate carboxylase and malic enzyme were measured in cell extracts from bacteria grown on the sugar indicated as the sole carbon source, as explained in Materials and Methods. The values of the corresponding enzymatic activities are shown in units per milligram of protein (U/mg protein). The bars represent the means for ≥6 independent biological replicates. Note that enzymatic activities were systematically higher in the *ptsN* and *ptsN ptsO* strains than in the wild type.

PtsN (or PtsN/PtsO), regardless of the carbon source employed for growth. This trend was also observed when the specific activity of the pyruvate carboxylase was measured in the extracts of the mutants; both increased with respect to the wild-type independ ently of the sugar present in the growth medium. These differences in key enzymes at the boundary of the upper and lower metabolic domains (Fig. 2) may suffice to explain the observed divergences of the corresponding fluxes reported above. Because transcription of *maeB*, *accC-2*, or *oadA* is not affected by the loss of PtsN (K. Pflüger-Grau et al., unpublished data), it is plausible that downregulation of the encoded enzymes is caused by direct protein-protein interactions, as is the rule for other PTS proteins (14, 18, 33).

The regulatory effects of PTS can be traced to the nonphosphorylated form of the EIIA^{Ntr} protein. The results presented thus far point to PtsN as the only constituent of the *P. putida* PTS that is consistently associated with the changes in the fluxes reported above, but these results do not reveal the possible mechanism(s) involved. Some orthologous PtsN proteins from other bacteria (e.g., *Salmonella* [33]) have been observed to control the activity of other proteins regardless of their phosphorylation state. However, the majority of cases where the issue has been examined (18, 34–36) reveal that the action of EIIA-type enzymes on target proteins depends on the phosphorylation state of a conserved His residue, which in *P. putida* is residue 68 of the primary amino acid sequence. While the data above did not shed any direct light on this question, a comparison of the metabolic behavior of the mutants with the known routes of high-energy phosphorus though the phosphotransferases of the system (Fig. 1) provided some hints. On the one hand, the presence of PtsN was associated with a less active pyruvate shunt, while the loss of the EIIA^{Ntr} protein led to the stimulation of such a metabolic node (see Fig. S2 and Fig. S3), regardless of any other accompanying or alternative mutations. On the other hand, because PtsN can be phosphorylated both by PtsO (NPr, itself phosphorylated by PtsP/EI^{Ntr}) (Fig. 1) and by FruB (21), any of the strains bearing single *fruB* or *ptsP* mutations still generate a pool of phosphorylated and nonphosphorylated EIIA^{Ntr} proteins (21). However, the *ptsP fruB* mutant lacks any phosphotransferase able to target the H68 residue of PtsN, and therefore, EIIA^{Ntr} is kept entirely in a nonphosphorylated state (21). Because downregulation of the pyruvate shunt is maintained in the *ptsP fruB* strain (see Fig. S1), the logical conclusion is that the nonphosphorylated form of EIIA^{Ntr} is the cause of all regulatory effects observed. To test this hypothesis, we examined the activity of the malic enzyme as a proxy of all metabolic effects of EIIA^{Ntr} in a *P. putida* MAD2 derivative bearing an allele of *ptsN* [*ptsN*(*H68A*)] in which H68 of the protein had been changed to an alanine (34). *ptsN*(*H68A*) thus encodes a product comparable to the wild-type enzyme except that it cannot be phosphorylated. Replacements of His by Ala in phosphotranferases are generally considered to lock the corresponding protein in the nonphosphorylated state (31). The *P. putida ptsN*(*H68A*) strain possessed levels of malic enzyme activity as low as those of the wild type and clearly differentiated from those of the *ptsN* mutant (Fig. 5c and d), confirming that the nonphosphorylated form of EIIA^{Ntr} directly or indirectly downregulates this key step of the pyruvate shunt.

DISCUSSION

Unlike genetic networks, the functioning of which resembles circuits that follow a digital, binary logic (37, 38), metabolic networks are characterized by a type of homeostasis which prevents drastic responses to nutritional or environmental perturbations (30). Instead of the typical all-or-nothing behavior of the constituents of the bacterial transcriptome (30), biochemical networks are regulated by devices that tune, rather than switch, given metabolic regimes according to the overall physiological conditions. In the case of central metabolism, this process allows cells to generate the appropriate ratios of biosynthetic precursors to achieve balanced growth. Along with the allosteric regulation of enzymes and transcriptional factors by small molecules and metabolites (39), the PTS is recognized as an autonomous biochemical device that modulates a variety of cell functions in response to the intracellular PEP/pyruvate ratio (29), the presence of cognate sugars as growth substrates (8), the N/C ratio (40) and the intracellular/extracellular fraction of potassium ions (14, 18, 35). Given this background, we wanted to characterize the metabolic consequences of growing *P. putida* on either a PTS sugar (fructose) or a non-PTS counterpart (glucose).

Despite a structural similarity between the two hexoses and their close energy values, our data indicate that *P. putida* KT2440 metabolizes these two sugars through different metabolic routes. While glucose is consumed by many eubacteria through the typi-

cal glycolytic EMP pathway and only occasionally through the ED route (25), *P. putida* nearly exclusively employs the latter to metabolize this archetypal sugar (24) (see above). The EMP pathway is also disfavored in the case of fructose, as the greater portion of this carbohydrate is channeled into central metabolism through the ED enzymes as well. This comes as a surprise because, unlike glucose, *P. putida* has all the necessary enzymes to efficiently direct fructose metabolism through the standard and more thermodynamically favorable EMP route (28). However, a mere 34% of the upper C flow goes into glycolysis, compared to the majority, 52%, that runs through the ED pathway (Fig. 3). This paradox, which is not easy to explain, might be due to the environmental lifestyle of *P. putida* compared to typically glycolytic microorganisms, e.g., an increased demand of ED intermediates for constructing cell wall polymers and/or the increased demand for reduction equivalents (NADPH), the synthesis of which is favored in an ED regimen (41). Additionally, *P. putida* could use the ED route to rapidly earmark glucose for gluconate and thus sequester available carbon away from its competitors.

The differences between glucose and fructose utilization in the upper metabolic domain are reflected in the subsequent downstream reactions. As presented above, the flux of PEP→pyruvate, the activity of the pyruvate shunt, and the gluconeogenic reaction of OAA→PEP were more pronounced in cells grown on fructose than in their glucose-grown counterparts. The most salient difference was, in fact, the ~2.4-fold stimulation of the pyruvate shunt in cells grown on fructose. While the importance of this shunt in the metabolism of *Pseudomonas* has already been reported (24, 42), its biological role in this bacterium is puzzling. The two reactions involved in the shunt (malic enzyme and pyruvate carboxylase) result in a bypass that hydrolyzes ATP. Apparently futile metabolic reactions often behave as security valves for releasing carbon overflow (24, 43), an issue that, in the case of *P. putida*, deserves further study. Alternatively, this shunt might be a way to generate more NADPH, which again could be due to the lifestyle of *P. putida* and its requirements for more reducing equivalents. Regardless of such a biological function, fructose clearly stimulates various fluxes at the boundaries of the upper and the lower metabolic domains, or glucose represses them, resulting in the reported effects.

Given that both the EMP and the ED pathways ultimately produce the same intermediates (pyruvate and PEP) that feed the TCA cycle (Fig. 2), how is the operation of the upper metabolism transmitted to the downstream reactions? Because the major difference between glucose and fructose is their status as non-PTS and PTS sugars, respectively, we explored the effect of the corresponding phosphotransferases on the strength of the same pathway fluxes we studied with glucose versus fructose utilization. The results above reveal that (i) out of all the PTS proteins of *P. putida*, only PtsN ($EIIA^{Ntr}$) had a regulatory influence on the performance of central metabolic pathways, (ii) such an effect targets the activity of the pyruvate shunt, and (iii) strains expressing a nonphosphorylated form of $EIIA^{Ntr}$ display a lower activity of the malic enzyme. Therefore, the most plausible scenario is that the inhibitory action of PtsN is exerted by the nonphosphorylated protein. This scenario does not rule out the possibility that the same phosphotransferase may also have a scaffolding role in a multiprotein complex involving various metabolic enzymes (17, 34). The crucial question is, however, whether the metabolic effects of the nonphosphorylated form of $EIIA^{Ntr}$ and the enhancement of the pyruvate shunt in cells grown on fructose reflect the same regulatory event(s). As argued below, we advocate the view that they are closely related, if not largely equivalent, phenomena.

The phosphorylation state of PtsN has been demonstrated to depend both on PtsP and FruB (21) (Fig. 1). However, expression of the *fruBKA* operon in *P. putida* is under the strict control of the FruR (Cra) repressor (38), which is relieved only by fructose 1-phosphate (F1P), a compound that is produced exclusively in the presence of fructose (Fig. 1). When this PTS sugar is available, FruB is expressed, and PtsN can be phosphorylated by both PtsP and FruB. Glucose metabolism, in contrast, does not produce any F1P; thus, FruB is not expressed, and PtsN is amenable to phosphorylation by PtsP only. Our prediction is therefore that the pool of nonphosphorylated PtsN will be higher when grown on glucose because fructose induces an extra kinase activity (FruB) that increases the share of $EIIA^{Ntr}$ ~P. This is precisely what happens when *P. putida* cells grow exponentially in the presence of either glucose or fructose: the ratio of $EIIA/EIIA^{Ntr}$ ~P is higher than on the non-PTS sugar, while fructose leads to almost no accumulation of nonphosphorylated $EIIA^{Ntr}$ (21). If nonphosphorylated PtsN inhibits the pyruvate shunt, then somewhat similar effects could be obtained either by growing the cells on fructose or by simply deleting the *ptsN* gene. This is the trend observed in most of the data presented above. This explanation accounts for the phenomena reported in this work and pinpoints the PTS of *P. putida* as a key player in controlling such central metabolic transactions.

The results above do not indicate whether the regulatory action of PtsN on the biochemical reactions studied here is exerted directly through protein-protein interactions (as observed in many other cases with PTS proteins) (18, 33-35) or indirectly through changes in the levels of allosteric effectors of the relevant enzymes. Furthermore, the effects may not be limited to the PEP-Pyr-OAA node but may also extend to the entry of AcCoA into the TCA cycle by means of the enzyme pyruvate dehydrogenase (PDH). We have recently demonstrated that the nonphosphorylated form of $EIIA^{Ntr}$ binds the AceE component of PDH *in vitro*, downregulating its activity (34). Because some pyruvate carboxylases respond to AcCoA (42), the higher activity of the *P. putida* enzyme in the *ptsN* mutant reported above could stem from a higher conversion of pyruvate to AcCoA (reaction 11 in Fig. 2). Whatever the mechanism, the data presented above strengthen the view that the PTS is a key biochemical device for adjusting metabolic fluxes to satisfy the anabolic and energetic demands of the overall cell. Additionally, these results highlight the importance of posttranslational regulation of enzymatic networks, not just genetic control, for engineering *P. putida* cells as cell factories for the biotransformation or biodegradation of unusual substrates.

MATERIALS AND METHODS

Strains and media. All *Pseudomonas* strains used in this work were derived from *P. putida* MAD2 (44). This is a variant of the reference strain *P. putida* KT2440 inserted with a lacZ gene, which is otherwise irrelevant for the purpose of this work. All PTS mutants derived from *P. putida* MAD2 and employed in the experiments described below have been reported elsewhere (16, 45). These mutants were generated by inserting either a kanamycin (*km*) resistance gene or the *xylE* marker into *ptsP*, *ptsO*, *ptsN*, and *fruB*. The *ptsN*(*H68A*) strain employed for studying the effect of $EIIA^{Ntr}$ phosphorylation on activity of the malic enzyme was reported before (34). This mutant expresses a PtsN variant in which the phosphorylatable His-68 of the $EIIA^{Ntr}$ protein was replaced by an Ala residue as described previously (34). Unless indicated otherwise, cells

were grown at 30°C in synthetic mineral M9 medium (46) with 0.3% glucose or fructose as the sole carbon and energy source.

Growth conditions and analytical procedures. For the determination of physiological parameters, bacteria were cultured at 30°C in 500-ml baffled shake flasks with 50 ml of M9 medium with either glucose or fructose. Cell growth was monitored spectrophotometrically at 600 nm (OD_{600}), and sugar concentrations were determined enzymatically with the glucose (HK) assay kit (Sigma-Aldrich) and the D-fructose kit (Enzytec) according to the manufacturers' instructions. The following physiological parameters were determined using regression analysis during the exponential growth phase of the batch culture as described elsewhere (47): the maximum specific growth rate, the biomass yield on glucose or fructose, and specific glucose or fructose consumption. The correlation factors (k) between cell dry weight (CDW) and OD_{600} were determined from batch cultures of each mutant. CDWs were measured from at least four parallel 10-ml cell suspensions by harvesting the cells using fast filtration through preweighted nitrocellulose filters (0.45 μm), which were subsequently washed with 0.9% NaCl and dried at 105°C for 24 h to a constant weight.

Metabolic flux ratio analysis by GC-MS. Growth substrates were purchased from Sigma-Aldrich. To follow the metabolic fate of distinct atoms of glucose and fructose, cells were cultured in a medium with a unique substrate labeled only at carbon 1 (i.e., [1-^{13}C]glucose or [1-^{13}C]fructose). Alternatively, cells were also grown in a second medium containing a mixture of 20% uniformly labeled molecules ([U-^{13}C]glucose or [U-^{13}C]fructose) and 80% nonlabeled substrate (again, glucose or fructose). In either case, 5-ml cell aliquots were harvested at mid-exponential-phase growth using centrifugation at 1,200 × g and 4°C for 10 min. The pellet was washed twice with 1 ml of 0.9% NaCl and then hydrolyzed in 1 ml 6 M HCl for 24 h at 110°C in sealed 2-ml Eppendorf tubes. Samples were then desiccated overnight in a heating block at 85°C under a constant air stream. The hydrolysate was dissolved in 30 μl of 99.8% pure dimethyl formamide. For derivatization, 20 μl of *N*-methyl-*N*-(tert-butyldimethylsilyl)-trifluoroacetamide was added, and the mixture was incubated at 85°C for 60 min. The gas chromatography-mass spectrometry (GC-MS)-derived mass isotope distributions of proteinogenic amino acids were analyzed by injecting 1 μl of the derivatized sample into a gas chromatograph 6890 N (Agilent Technologies) combined with a mass-selective detector model 5973 (Agilent Technologies) and analyzed as described previously (48, 49). The corrected mass distributions were related to the *in vivo* metabolic activities obtained with previously described algebraic equations and statistical-data treatments of metabolic-flux ratio analysis (49) using the software Fiat Flux (50).

^{13}C-constrained metabolic net flux analysis. The metabolic model used for net flux analysis was based on the master reaction network (25) with some modifications in the upper metabolic domain for growth on fructose. In particular, we implemented the fact that, in *P. putida*, fructose is taken up by the PTS^{Fru} and directly activated to F1P, which is then converted to fructose 1,6-bisphosphate (FBP) by the activity of the 1-phosphofructokinase FruK (23, 28, 51–55) (Fig. 2). Net fluxes were calculated using (i) the stoichiometric reaction matrix, (ii) the METAFoR analysis-derived flux ratios, (iii) physiological data, and (iv) precursor requirements for biomass synthesis as described previously (50). Specifically, the following flux ratios were considered: serine derived from the Embden-Meyerhof-Parnas (EMP) pathway, pyruvate derived from the Entner-Doudoroff (ED) pathway, oxaloacetate (OAA) derived from pyruvate, phosphoenolpyruvate (PEP) derived from OAA, the lower and upper bounds of pyruvate derived from malate, and the upper bound of PEP derived from the pentose phosphate (PP) pathway. The stoichiometric matrix was then solved with the MatLab-based program Netto of the Fiat Flux software (50) using both metabolite balances and flux ratios to obtain the estimated net fluxes.

Measurement of enzymatic activities. Crude cell extracts for *in vitro* enzyme assays were prepared as follows. After reaching the exponential phase, 50-ml cultures of the strains of interest were harvested using centrifugation (15 min, 4,000 × g, 4°C). The pellets were then resuspended in phosphate-buffered saline buffer (1×) to a concentration equivalent to that of a 25-ml culture at an OD_{600} of 0.8 per ml of suspension. The cells were sonicated on ice and spun down for 30 min at 14,000 × g to collect the debris. The protein concentrations of the supernatants were measured using the Bradford assay (56) before use in enzymatic assays. The NADP-dependent malic enzyme was assayed as described elsewhere (57). The reaction mixture (200 μl) contained 25 μg of cell extract in a buffer with 67 mM triethanolamine, 3.3 mM l-malic acid, 0.3 mM β-NADP, and 5.0 mM magnesium chloride. The specific activity was monitored spectrophotometrically: the increase in 340-nm absorbance at 25°C due to NADPH production was followed for 10 min in a 200-μl well plate with the Victor2 multitasking plate reader (PerkinElmer). The enzymatic activities were then calculated as micromoles of substrate converted per milligram of protein per minute (U/mg protein). The pyruvate carboxylase assays (58) were run similarly in a 200-μl volume containing 75 μg of cell protein extract in a buffer with 134 mM triethanolamine, 5 mM magnesium sulfate, 7 mM pyruvic acid, 0.12% (wt/vol) bovine serum albumin, 0.23 mM β-NADH, 0.05 mM acetyl coenzyme A, 2.63 U malic dehydrogenase (Sigma Aldrich), 1 mM adenosine 5'-triphosphate, 15 mM potassium bicarbonate, 0.05% (vol/vol) glycerol, 0.002 mM magnesium acetate, 0.001 mM EDTA, and 0.05 mM Tris-HCl. The decrease in absorbance at 340 nm due to NADH consumption at 25°C was followed for 10 min, and the units were expressed in μmol of substrate converted/mg protein/min (U/mg protein) as before.

ACKNOWLEDGMENTS

This work was supported by the BIO and FEDER CONSOLIDER-INGENIO program of the Spanish Ministry of Science and Innovation, the BACSINE and MICROME Contracts of the EU, and the funds of the Autonomous Community of Madrid. Max Chavarría is grateful to the Universidad de Costa Rica and the CSIC for a joint collaborative PhD stipend.

SUPPLEMENTAL MATERIAL

Supplemental material for this article may be found at http://mbio.asm.org/lookup/suppl/doi:10.1128/mBio.00028-12/-/DCSupplemental.

Figure S1, PDF file, 0.6 MB.
Figure S2, PDF file, 0.5 MB.
Figure S3, PDF file, 0.5 MB.

REFERENCES

1. **Holms H.** 1996. Flux analysis and control of the central metabolic pathways in *Escherichia coli*. FEMS Microbiol. Rev. **19**:85–116.
2. **Perrenoud A, Sauer U.** 2005. Impact of global transcriptional regulation by ArcA, ArcB, Cra, Crp, Cya, Fnr, and Mlc on glucose catabolism in *Escherichia coli*. J Bacteriol **187**:3171–3179.
3. **Gerosa L, Sauer U.** Regulation and control of metabolic fluxes in microbes. Curr. Opin. Biotechnol. **22**:566–575.
4. **Görke B, Vogel J.** 2008. Noncoding RNA control of the making and breaking of sugars. Genes Dev. **22**:2914–2925.
5. **Saier MH, Jr, Chauvaux S, Deutscher J, Reizer J, Ye JJ.** 1995. Protein phosphorylation and regulation of carbon metabolism in Gram-negative versus Gram-positive bacteria. Trends Biochem. Sci. **20**:267–271.
6. **Stock JB, Ninfa AJ, Stock AM.** 1989. Protein phosphorylation and regulation of adaptive responses in bacteria. Microbiol. Rev. **53**:450–490.
7. **Deutscher J, Francke C, Postma PW.** 2006. How phosphotransferase system-related protein phosphorylation regulates carbohydrate metabolism in bacteria. Microbiol. Mol. Biol. Rev. **70**:939–1031.
8. **Postma PW, Lengeler JW, Jacobson GR.** 1993. Phosphoenolpyruvate: carbohydrate phosphotransferase systems of bacteria. Microbiol. Rev. **57**:543–594.
9. **Saier MH, Jr, Reizer J.** 1994. The bacterial phosphotransferase system: new frontiers 30 years later. Mol. Microbiol. **13**:755–764.
10. **Tchieu JH, Norris V, Edwards JS, Saier MH, Jr.** 2001. The complete phosphotransferase system in *Escherichia coli*. J. Mol. Microbiol. Biotechnol. **3**:329–346.
11. **Barabote RD, Saier MH, Jr.** 2005. Comparative genomic analyses of the

bacterial phosphotransferase system. Microbiol. Mol. Biol. Rev. **69**: 608–634.
12. **Reizer J, Reizer A, Saier MH, Jr, Jacobson GR.** 1992. A proposed link between nitrogen and carbon metabolism involving protein phosphorylation in bacteria. Protein Sci. **1**:722–726.
13. **Pflüger-Grau K, Görke B.** 2010. Regulatory roles of the bacterial nitrogen-related phosphotransferase system. Trends Microbiol. **18**: 205–214.
14. **Lee CR, Cho SH, Yoon MJ, Peterkofsky A, Seok YJ.** 2007. *Escherichia coli* enzyme IIA^{Ntr} regulates the K^+ transporter TrkA. Proc. Natl. Acad. Sci. U. S. A. **104**:4124–4129.
15. **Powell BS, et al.** 1995. Novel proteins of the phosphotransferase system encoded within the *rpoN* operon of *Escherichia coli*. Enzyme IIA^{Ntr} affects growth on organic nitrogen and the conditional lethality of an erats mutant. J. Biol. Chem. **270**:4822–4839.
16. **Cases I, Pérez-Martín J, de Lorenzo V.** 1999. The IIA^{Ntr} (PtsN) protein of *Pseudomonas putida* mediates the C source inhibition of the sigma54-dependent *Pu* promoter of the TOL plasmid. J. Biol. Chem. **274**: 15562–15568.
17. **Cases I, Lopez JA, Albar JP, de Lorenzo V.** 2001. Evidence of multiple regulatory functions for the PtsN (IIA(Ntr)) protein of *Pseudomonas putida*. J. Bacteriol. **183**:1032–1037.
18. **Lüttmann D, et al.** 2009. Stimulation of the potassium sensor KdpD kinase activity by interaction with the phosphotransferase protein IIA(Ntr) in *Escherichia coli*. Mol. Microbiol. **72**:978–994.
19. **Velázquez F, Pflüger K, Cases I, De Eugenio LI, de Lorenzo V.** 2007. The phosphotransferase system formed by PtsP, PtsO, and PtsN proteins controls production of polyhydroxyalkanoates in *Pseudomonas putida*. J. Bacteriol. **189**:4529–4533.
20. **Cases I, Velázquez F, de Lorenzo V.** 2007. The ancestral role of the phosphoenolpyruvate-carbohydrate phosphotransferase system (PTS) as exposed by comparative genomics. Res. Microbiol. **158**:666–670.
21. **Pflüger K, de Lorenzo V.** 2008. Evidence of *in vivo* cross talk between the nitrogen-related and fructose-related branches of the carbohydrate phosphotransferase system of *Pseudomonas putida*. J. Bacteriol. **190**: 3374–3380.
22. **Zimmer B, Hillmann A, Görke B.** 2008. Requirements for the phosphorylation of the *Escherichia coli* $EIIA^{Ntr}$ protein *in vivo*. FEMS Microbiol. Lett. **286**:96–102.
23. **Velázquez F, di Bartolo I, de Lorenzo V.** 2004. Genetic evidence that catabolites of the Entner-Doudoroff pathway signal C source repression of the sigma54 *Pu* promoter of *Pseudomonas putida*. J. Bacteriol. **186**: 8267–8275.
24. **del Castillo T, et al.** 2007. Convergent peripheral pathways catalyze initial glucose catabolism in *Pseudomonas putida*: genomic and flux analysis. J. Bacteriol. **189**:5142–5152.
25. **Fuhrer T, Fischer E, Sauer U.** 2005. Experimental identification and quantification of glucose metabolism in seven bacterial species. J. Bacteriol. **187**:1581–1590.
26. **Nogales J, Palssøn BO, Thiele I.** 2008. A genome-scale metabolic reconstruction of *Pseudomonas putida* KT2440: iJN746 as a cell factory. BMC Syst. Biol. **2**:79.
27. **Puchalka J, et al.** 2008. Genome-scale reconstruction and analysis of the *Pseudomonas putida* KT2440 metabolic network facilitates applications in biotechnology. PLoS Comput. Biol. **4**:e1000210.
28. **Van Dijken JP, Quayle JR.** 1977. Fructose metabolism in four *Pseudomonas* species. Arch. Microbiol. **114**:281–286.
29. **Sauer U, Eikmanns BJ.** 2005. The PEP-pyruvate-oxaloacetate node as the switch point for carbon flux distribution in bacteria. FEMS Microbiol. Rev. **29**:765–794.
30. **Grüning NM, Lehrach H, Ralser M.** 2010. Regulatory crosstalk of the metabolic network. Trends Biochem. Sci. **35**:220–227.
31. **Pflüger K, de Lorenzo V.** 2007. Growth-dependent phosphorylation of the PtsN (EII^{Ntr}) protein of *Pseudomonas putida*. J. Biol. Chem. **282**: 18206–18211.
32. **Eyzaguirre J, Cornwell E, Borie G, Ramírez B.** 1973. Two malic enzymes in *Pseudomonas aeruginosa*. J. Bacteriol. **116**:215–221.
33. **Choi J, et al.** 2010. *Salmonella* pathogenicity island 2 expression negatively controlled by $EIIA^{Ntr}$-SsrB interaction is required for *Salmonella* virulence. Proc. Natl. Acad. Sci. U. S. A. **107**:20506–20511.
34. **Pflüger-Grau K, Chavarría M, de Lorenzo V.** 2011. The interplay of the EIIA(Ntr) component of the nitrogen-related phosphotransferase system (PTS(Ntr)) of *Pseudomonas putida* with pyruvate dehydrogenase. Biochim. Biophys. Acta **1810**:995–1005.
35. **Lee CR, et al.** 2005. Requirement of the dephospho-form of enzyme IIA^{Ntr} for derepression of *Escherichia coli* K-12 *ilvBN* expression. Mol. Microbiol. **58**:334–344.
36. **Begley GS, Jacobson GR.** 1994. Overexpression, phosphorylation, and growth effects of ORF162, a *Klebsiella pneumoniae* protein that is encoded by a gene linked to *rpoN*, the gene encoding sigma 54. FEMS Microbiol. Lett. **119**:389–394.
37. **Silva-Rocha R, de Lorenzo V.** 2010. Noise and robustness in prokaryotic regulatory networks. Annu. Rev. Microbiol. **64**:257–275.
38. **Chavarría M, et al.** 2011. Fructose 1-phosphate is the preferred effector of the metabolic regulator cra of *Pseudomonas putida*. J. Biol. Chem. **286**: 9351–9359.
39. **Camilli A, Bassler BL.** 2006. Bacterial small-molecule signaling pathways. Science **311**:1113–1116.
40. **Commichau FM, Forchhammer K, Stülke J.** 2006. Regulatory links between carbon and nitrogen metabolism. Curr. Opin. Microbiol. **9**:167–172.
41. **Conway T.** 1992. The Entner-Doudoroff pathway: history, physiology and molecular biology. FEMS Microbiol. Rev. **9**:1–27.
42. **Diesterhaft MD, Freese E.** 1973. Role of pyruvate carboxylase, phosphoenolpyruvate carboxykinase, and malic enzyme during growth and sporulation of *Bacillus subtilis*. J. Biol. Chem. **248**:6062–6070.
43. **Portais JC, Delort AM.** 2002. Carbohydrate cycling in micro-organisms: what can ^{13}C-NMR tell us? FEMS Microbiol. Rev. **26**:375–402.
44. **Fernández S, de Lorenzo V, Pérez-Martín J.** 1995. Activation of the transcriptional regulator XylR of *Pseudomonas putida* by release of repression between functional domains. Mol. Microbiol. **16**:205–213.
45. **Cases I, Velázquez F, de Lorenzo V.** 2001. Role of *ptsO* in carbon-mediated inhibition of the *Pu* promoter belonging to the pWW0 *Pseudomonas putida* plasmid. J. Bacteriol. **183**:5128–5133.
46. **Miller JH.** 1972. Experiments in molecular genetics. Cold Spring Harbor, New York, NY.
47. **Sauer U, et al.** 1999. Metabolic flux ratio analysis of genetic and environmental modulations of *Escherichia coli* central carbon metabolism. J. Bacteriol. **181**:6679–6688.
48. **Dauner M, Sauer U.** 2000. GC-MS analysis of amino acids rapidly provides rich information for isotopomer balancing. Biotechnol. Prog. **16**: 642–649.
49. **Fischer E, Sauer U.** 2003. Metabolic flux profiling of *Escherichia coli* mutants in central carbon metabolism using GC-MS. Eur. J. Biochem. **270**:880–891.
50. **Zamboni N, Fischer E, Sauer U.** 2005. FiatFlux—a software for metabolic flux analysis from 13C-glucose experiments. BMC Bioinformatics. **6**:209.
51. **Lessie TG, Phibbs PV, Jr.** 1984. Alternative pathways of carbohydrate utilization in pseudomonads. Annu. Rev. Microbiol. **38**:359–388.
52. **Schleissner C, Reglero A, Luengo JM.** 1997. Catabolism of D-glucose by *Pseudomonas putida* U occurs via extracellular transformation into D-gluconic acid and induction of a specific gluconate transport system. Microbiology **143**:1595–1603.
53. **Sawyer MH, et al.** 1977. Pathways of D-fructose catabolism in species of *Pseudomonas*. Arch. Microbiol. **112**:49–55.
54. **Vicente M, Cánovas JL.** 1973. Glucolysis in *Pseudomonas putida*: physiological role of alternative routes from the analysis of defective mutants. J. Bacteriol. **116**:908–914.
55. **Vicente M.** 1975. The uptake of fructose by *Pseudomonas putida*. Arch. Microbiol. **102**:163–166.
56. **Bradford MM.** 1976. A rapid and sensitive method for the quantitation of microgram quantities of protein utilizing the principle of protein-dye binding. Anal. Biochem. **72**:248–254.
57. **Geer BW, Krochko D, Williamson JH.** 1979. Ontogeny, cell distribution, and the physiological role of NADP-malic enxyme in *Drosophila melanogaster*. Biochem. Genet. **17**:867–879.
58. **Warren GB, Tipton KF.** 1974. Pig liver pyruvate carboxylase. The reaction pathway for the decarboxylation of oxaloacetate. Biochem. J. **139**: 321–329.